Semicond. Sci. Technol. 10 (1995) 1413–1417. Printed in the UK

LETTER TO THE EDITOR

Antidot superlattices in two-dimensional hole gases confined in strained germanium layers

D Többen†‡, M Holzmann†, G Abstreiter†, A Kriele§, H Lorenz§, J P Kotthaus§, F Schäffler‖, Y H Xie¶, P J Silverman¶ and Don Monroe¶

† Walter Schottky Institute, Technische Universität München, D-85748 Garching, Germany
§ Sektion Physik der Ludwig-Maximilians-Universität München, Geschwister-Scholl-Platz 1, D-80539 München, Germany
‖ Daimler-Benz AG, Forschungsinstitut Ulm, Wilhelm-Runge-Str. 11, D-89081 Ulm, Germany
¶ AT&T Bell Laboratories, Murray Hill, NJ 07974, USA

Received 5 May 1995, in final form 10 July 1995, accepted for publication 20 July 1995

Abstract. Antidot superlattices with a period of $a = 500$ nm and different etch depths were fabricated in two-dimensional hole gases confined in surface-side as well as in substrate-side modulation-doped Ge/SiGe heterostructures by holographic lithography and reactive ion etching and were then studied by magnetotransport at $T = 4.2$ K. Even though the elastic mean free paths are smaller than or comparable to the superlattice period, typical features of locally ballistic transport around groups of antidots, such as commensurability oscillations and additional, non-quantized Hall plateaus, are observed in both types of samples at sufficient etch depth. These geometry-related effects are found to be rather robust against inhomogeneities and defects brought about by imperfect fabrication.

Antidot superlattices have attracted much attention both experimentally [1–4] and theoretically [5, 6] as a means of purposely introducing scatterers into a conducting system in an ordered manner and of studying locally ballistic transport. The lateral potential modulation leads to a number of magnetotransport effects, most of which can be understood in terms of a semiclassical, single-particle picture when a certain smoothness of the antidot potential is taken into account. Commensurability oscillations in the longitudinal resistivity ρ_{xx} and additional non-quantized Hall plateaus, for example, are associated with trajectories whirling around groups of antidots [5], while quenching of the Hall effect around $B = 0$ arises from carriers which are channelled by the superlattice for many periods and which are then scattered in a direction opposite to the Lorentz force [6].

Various fabrication techniques have been successfully employed, but so far all experiments have been almost exclusively performed with high-mobility two-dimensional electron gases (2DEGs) in GaAs/AlGaAs heterostructures because the elastic mean free path $l_{\mathrm{mfp}} = \hbar\mu\sqrt{4\pi n_s/g_s g_v}/e$ has to be larger than the superlattice period in order to see a pronounced effect. Here, μ, n_s, g_s and g_v are the mobility, carrier density, spin degeneracy and valley degeneracy respectively of the 2DEG. Very recently, the typical phenomena mentioned above have also been reported for n-type modulated-doped Si/SiGe heterostructures with antidot superlattices fabricated by reactive ion etching (RIE) and field-effect induction via a patterned gate [7, 8].

The ballistic transport regime is generally much more easily accessible when one is experimenting with electron rather than with hole gases because of the enhanced mobility. In this work, however, we report on magnetotransport studies performed on antidot superlattices fabricated in two-dimensional hole gases (2DHGs) which are confined in strained Ge/SiGe heterostructures. In the Si/Ge material system such 2DHGs have recently attracted a lot of attention as a possible candidate for high-performance p-channels in complementary modulation-doped field-effect transistor (CMODFET) logics [9]. Both heterostructures we used were deposited on relaxed, graded SiGe buffer layers several micrometres thick grown on Si (100) substrates by molecular beam epitaxy (MBE). Thus, the Ge channels

‡ Present address: Siemens AG, Otto-Hahn-Ring 6, HL PES 31, D-81739 München, Germany.

0268-1242/95/101413+05$19.50

containing the 2DHGs are under compressive strain. The degeneracy of the valence band at $\boldsymbol{k} = 0$ is thereby lifted and the $|3/2, \pm 3/2\rangle$ states become lowest in energy.

Structure A was grown at Daimler-Benz. Details on growth and magnetotransport work have been published in [9, 10]. The final Ge content of the buffer is about 80% as determined by x-ray rocking analysis. The strained 17 nm thick Ge layer is situated 65 nm beneath the surface and separated from the surface-side gallium modulation doping (integral density about 5×10^{12} cm^{-2}) by a 17 nm thick $Si_{0.4}Ge_{0.6}$ spacer layer.

Structure B was fabricated at AT&T Bell Laboratories as described in [11]. A rather complex layer sequence involving several doped layers was deposited on top of the graded $Si_{0.4}Ge_{0.6}$ buffer layer before the Ge/SiGe heterostructure itself was grown. Because of the inherent tendency of three-dimensional (3D) growth of the Ge channel the sample was substrate-side modulation-doped to ensure that the 2DHG is generated at the high-quality Ge/SiGe interface. Important parameters for lateral patterning efforts by RIE are the positions of the two Ge/SiGe interfaces, 73 nm and 88 nm beneath the surface, respectively, and of the boron δ-doping (1.1×10^{12} cm^{-2}), 108 nm beneath the surface. To saturate the surface band bending, an additional δ-doping spike (1.6×10^{12} cm^{-2}) was placed at a depth of 20 nm.

Antidot superlattices with a period of $a = 500$ nm were fabricated by holographic lithography and subsequent RIE with CF_4 as described previously [7]. Etch depth and lithographic antidot size were determined by atomic force microscopy (AFM) after removal of the photoresist. Using structure A, superlattices with etch depths $z_{RIE} = 45$ nm, 73 nm and 100 nm (hereafter referred to as A1–A3) were realized. The antidots thus extend into the gallium doping layer, into the Ge channel, and well into the buffer layer respectively. Two antidot superlattices were fabricated from structure B with etch depths of 66 nm and 101 nm (hereafter referred to as B1 and B2). Thus, the Ge channel is still intact in the less deeply etched specimen, while it has been completely removed in the antidots of the other one. Because of the long etch duration, sample B2 was also slightly etched (18 nm) in the regions between two adjacent antidots. However, since the top doping spike was not yet etched and based on the results discussed below it is reasonable to assume that this has no negative influence on the measurements.

Figure 1 shows AFM images of the patterned surfaces of samples A2 and B1 and simultaneously illustrates one of the main problems of this material system which may arise in nanometre-scale lithography. Strong inhomogeneity of the antidot diameters is obvious for sample A2. Because of the surface undulation which is typical for heterostructures grown on relaxed SiGe buffers [12], the nominally 90 nm thick photoresist film cannot be spun onto the sample homogeneously and the holographic double exposure leads to larger voids in those regions with reduced resist thickness. Sample B2, on the other hand, is covered with a much more regular array of antidots as a result of an intermediate planarization process which renders a flatter surface. The average antidot diameter is around

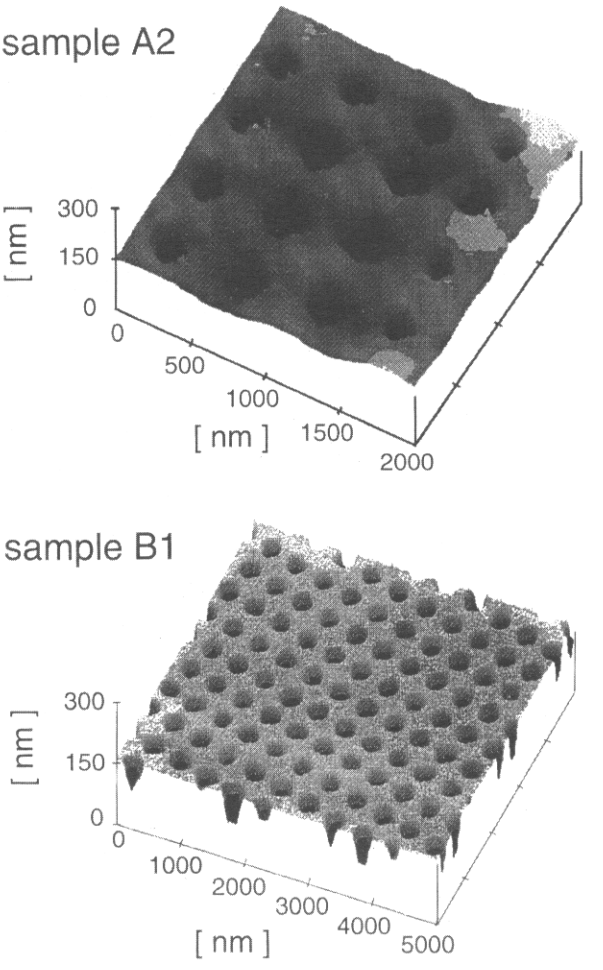

Figure 1. Atomic force microscope images of the surfaces of samples A2 with an etch depth $z_{RIE} = 73$ nm and B1 with $z_{RIE} = 66$ nm. The superlattice period is $a = 500$ nm in both cases. The inhomogeneities of the antidot diameters on sample A2 arise during the holographic lithography due to strong surface undulation.

50% of the superlattice period in all patterned samples, similar to the values obtained previously with holographic lithography [7].

Mesas in Hall bar geometry with active areas of 80×400 μm^2 were defined afterwards by standard optical lithography and wet chemical etching, before ohmic contacts of Al and Au were deposited and alloyed. All measurements were performed in a bath cryostat at $T = 4.2$ K using a direct current of 1 μA. Unpatterned references of structures A and B yield mobilities of $\mu = 15\,500$ cm^2 V^{-1} s^{-1} and $40\,000$ cm^2 V^{-1} s^{-1} at carrier densities of $p_s = 1.09 \times 10^{12}$ cm^{-2} and 0.64×10^{12} cm^{-2} respectively. Hence, the elastic mean free paths in the two structures are determined to be 0.26 μm and 0.53 μm respectively. Here, the ratio of l_{mfp} and a is barely of the order of one and is thus clearly less than for 2DEGs in GaAs/AlGaAs or Si/SiGe heterostructures [1–4, 7, 8].

Figure 2(a) shows the longitudinal resistivity ρ_{xx} of the three antidot superlattices fabricated from structure A and of an unpatterned reference in the dark as a function of the magnetic field. Illumination with a red light-emitting diode (LED) caused hardly any changes in the data. As expected, the zero-field resistivity increases with increasing

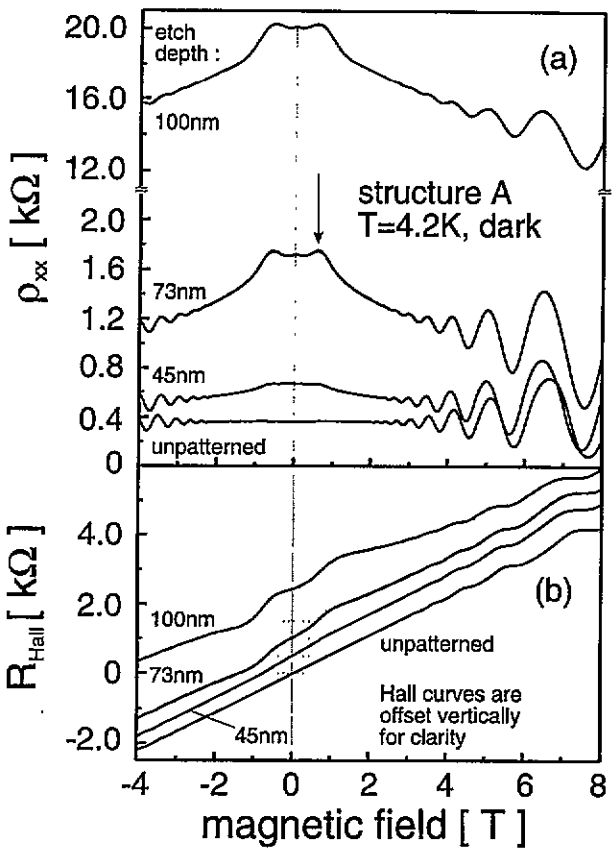

Figure 2. (*a*) Longitudinal resistivity and (*b*) Hall resistance of samples A1–A3 and an unstructured reference at $T = 4.2$ K. The Hall curves are offset vertically for clarity. The arrow marks the commensurability peak associated with ballistic motion around a single antidot.

etch depth. Note the different scale on the vertical axis for the most deeply etched sample A3. At higher fields, i.e. $B \geq 2$ T, the onset of Shubnikov–de Haas (SdH) oscillations is observed. This regime was used to evaluate the carrier density p_s, which is the same in all specimens except for sample A1 yielding $p_s = 1.07 \times 10^{12}$ cm^{-2}.

In the low-field regime around $B \approx 0.6$ T there is an additional feature, i.e. a shoulder in sample A1 and a distinct peak in samples A2 and A3, which is marked by the arrow in figure 2(*a*). All curves are symmetric towards reversal of the magnetic field. Evaluating the cyclotron radius $r_c = \hbar\sqrt{4\pi p_s/g_s g_v}/eB$ at the peak positions yields $r_c/a \approx 0.51$, 0.59 and 0.61 for samples A1–A3 respectively. We interpret this feature to arise from ballistic motion around a single antidot even though one would expect r_c/a to be equal to 0.5 [2,5]. Obviously, one has to etch beyond the doping layer to generate a strong lateral potential. Very deep etching, on the other hand, results in drastic reduction of the conductivity. One of the potential probes on the A3 Hall bar was even totally depleted. The observation of a commensurability maximum in these samples is rather astonishing since the superlattice period exceeds the mean free path by about a factor of two. The shift of the peaks to smaller magnetic fields than expected in our data might be due to an increased softness of the potential and to different carrier densities in the deeply etched samples A2 and A3: the periodicity of the SdH oscillations at high magnetic fields is determined by p_s in the relatively undisturbed 2DHG still present between four antidots. However, the Fermi energy is lowered in the saddle-shaped potential between two antidots, leading to a reduction of the carrier density in this region, which is important at low magnetic fields.

The corresponding Hall traces of these samples are displayed in figure 2(*b*). The curves have been offset vertically by 0.5 kΩ each for clarity. As the etch depth is increased, deviations from the linear dependence of the Hall resistance R_{Hall} on B around zero field and an additional plateau become more and more pronounced. At $B = 0$, we have measured an offset value of about 0.8 kΩ in sample A3, presumably resulting from inhomogeneities in this very deeply etched sample. However, the symmetry towards the intercept with the vertical axis is clearly recognizable, and we thus believe that the influence of the etched antidot superlattice is reflected in a qualitatively correct manner.

Alternative explanations for the observed magnetotransport anomalies might be trapping of electrons between four antidots [13] or diffusive backscattering [14] associated with channelling of charge carriers in a certain direction of the superlattice due to its inhomogeneity. In the latter case, however, the ratio r_c/a would shrink with increasing z_{RIE} as the effective channel width $W \approx 0.55 r_c$ is reduced [14]. The opposite is observed in the experiments. For electrostatically defined superlattices in GaAs/AlGaAs structures with large antidot diameters the low-field magnetoresistance maximum, which was observed in samples with resistivities of the order $h/2e^2$, was ascribed to a trajectory between four antidots rather than around a single one since the constrictions of the superlattice can then be regarded as point contacts [13]. The resistivity of sample A3 is also of the order of h/e^2. However, our antidots are not as large compared with the superlattice period and there is no enhancement of the SdH amplitudes as reported in [13], leading us to dismiss this interpretation as well. The shape of the upper two curves in figure 1 is reminiscent of data recently reported by Müller *et al* [15] in 2DEGs with an imposed one-dimensional (1D) periodic potential of intermediate modulation strength and referred to as a 'spiked-helmet'-like commensurability structure followed by a pronounced resistance drop as B was increased. The authors explained their experimental findings by changes in the carrier densities and simultaneously in the scattering rates at the top and the bottom of the potential landscape. This situation is, of course, somewhat similar to the possible reduction of the carrier density between two antidots as mentioned above: one might indeed consider the holes to travel in an effective 1D potential, rather than on circular orbits around the antidots. Even if this scenario explained the shape of the ρ_{xx} data, it would, however, fail to account for the pronounced Hall effect anomalies.

The appearance of the typical non-quantized Hall plateau at the same magnetic field as the anomalous feature in ρ_{xx} and the onset of quenching of the Hall effect around $B = 0$ further support our interpretation that this magnetoresistance maximum is indeed a commensurability peak associated with motion around a single antidot in

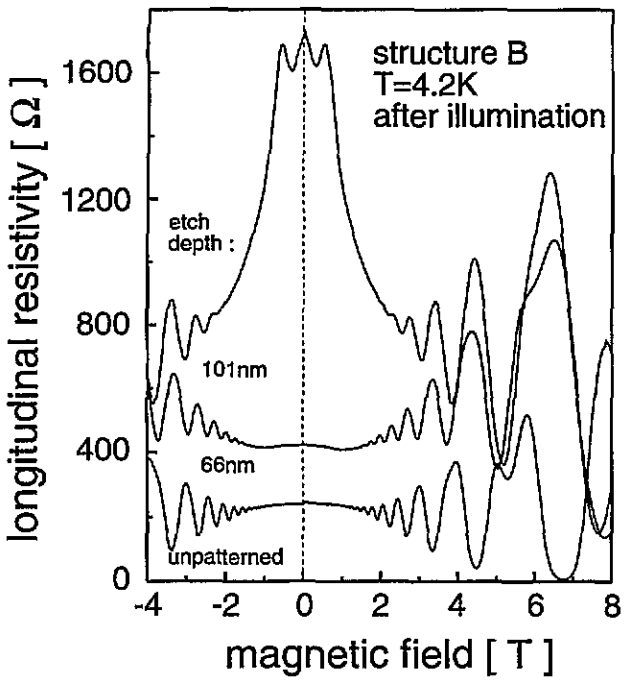

Figure 3. Longitudinal resistivity of samples B1, B2 and an unstructured reference at $T = 4.2$ K.

spite of the relatively small mean free path and the inhomogeneity of the antidot superlattice. It should also be noted that the relative peak amplitudes $\Delta\rho_{xx}/\rho_{xx}(B = 0)$ are only 2.3% and 1.2% for samples A2 and A3 respectively. Values around 20% were reported for 2DEGs in Si/SiGe heterostructures [7]. Since the elastic mean free path is a statistical quantity it is reasonable to assume that a few holes will be capable of travelling without collision around an antidot. The resistivity of sample A3, which is of the order of h/e^2 at $B = 0$, indicates the presence of strongly depleted regions in the superlattice which only contribute to a large serial background resistance rather than to a commensurability effect.

Structure B appears to be a more promising candidate for this kind of experiment because l_{mfp} is at least as large as the superlattice period a. Also, the surface is much smoother and the imposed array of antidots is thus much more homogeneous. However, the generation of a strong lateral potential with simultaneous conservation of the high hole mobility might be complicated by the fact that the 2DHG is situated at the substrate-side interface. All data shown here were taken after intense illumination with a red LED because the samples thereby appeared to become more homogeneous even though the resisitivites and the carrier densities were only weakly affected. Figure 3 shows the longitudinal resistivities of samples B1, B2 and an unpatterned reference versus the magnetic field. The traces look very similar to those of figure 2, although the resistivity remains well below h/e^2 even in the very deeply etched sample B2. It is noteworthy, though, that the carrier density is enhanced to $p_s = 0.70 \times 10^{12}$ cm^{-2} and $p_s = 0.75 \times 10^{12}$ cm^{-2} in samples B1 and B2 respectively.

Sample B2 yields a distinct magnetoresistance peak in the low-field regime while there is only a vague kink observable at close inspection in the data taken from

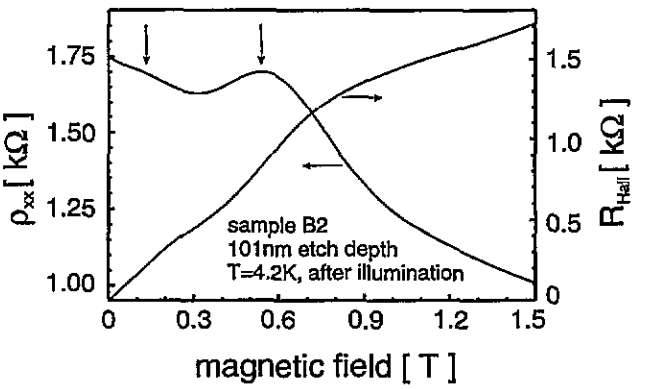

Figure 4. Longitudinal resistivity and Hall resistance of sample B2 at low magnetic fields. Two commensurability features are observable in both ρ_{xx} and R_{Hall} as marked by the vertical arrows.

sample B1. Both features appear at $r_c/a \approx 0.53$, i.e. very close to the value expected for a commensurability maximum. Because of the substrate-side doping employed in structure B one obviously has to etch rather deeply into the semiconductor in order to observe an influence of the antidot superlattice other than an increase in the sample resistance. It is indeed very interesting to note that the hole mobility appears to remain relatively unaffected in spite of the fact that we have physically cut through the 2DHG, a process commonly referred to as deep etching. A reduction of the sample quality can only be deduced from the fact that the resolution of the lifted spin degeneracy around $B \approx 5$–6 T becomes less pronounced with increasing z_{RIE}.

As a matter of fact, an additional peak-like structure in ρ_{xx} is observable at $B \approx 0.15$ T in sample B2 as marked by the vertical arrows in figure 4. Just as the main maximum, it is accompanied by the onset of a further plateau in R_{Hall}. These features arise from the ballistic motion of holes around four antidots. Their appearance as well as the increased relative height of the main peak, $\Delta\rho_{xx}/\rho_{xx}(B = 0) = 4.0\%$, as compared to those observed in samples fabricated from structure A, are a direct consequence of the larger mean free path of the 2DHG confined in structure B as well as of the smoother surface.

In conclusion, we have used RIE to fabricate antidot superlattices in 2DHGs in both surface and substrate-side modulation-doped Ge/SiGe heterostructures. Even though the elastic mean free paths are smaller than or just comparable to the superlattice period typical magnetotransport anomalies associated with collision-free trajectories around a single and even four antidots have been observed. These effects are therefore not as pronounced as in electron systems. However, they appear to be very robust against inhomogeneities in the artificial array of scatterers caused by the surface undulation. Also, we have shown that even a very deep RIE process preserves the intrinsic sample quality.

We thank S Kühn for technological support with the sample preparation. This work was supported financially in part by the Siemens AG (SFE Mikrostrukturierte Bauelemente) and by the Bundesministerium für Bildrung, Wissenschaft, Forschung und Technologie (Bonn, Germany) under grant NT 24137.

References

[1] Ensslin K and Petroff P M 1990 *Phys. Rev.* B **41** 12 307

[2] Weiss D, Roukes M L, Menschig A, Grambow P, von Klitzing K and Weimann G 1991 *Phys. Rev. Lett.* **66** 2790

[3] Lorke A, Kotthaus J P and Ploog K 1991 *Phys. Rev.* B **44** 3447

[4] Weiss D, Richter K, Menschig A, Bergmann R, Schweizer H, von Klitzing K and Weimann G 1993 *Phys. Rev. Lett.* **70** 4118

[5] Fleischmann R, Geisel T and Ketzmerick R 1992 *Phys. Rev. Lett.* **68** 1367

[6] Fleischmann R, Geisel T and Ketzmerick R 1994 *Europhys.Lett.* **25** 219

[7] Többen D, Holzmann M, Kühn S, Lorenz H, Abstreiter G, Kotthaus J P and Schäffler F 1994 *Phys. Rev.* B **50** 8853

[8] Többen D, Holzmann M, Kühn S, Lorenz H, Abstreiter G, Kotthaus J P and Schäffler F 1995 *Proc. 11th Int. Conf. on High Magnetic Fields in Semiconductor Physics (Boston, 1994)* (Singapore: World Scientific) at press

[9] König U and Schäffler F 1993 *IEEE Electron Device Lett.* **14** 205

[10] Engelhardt C M, Többen D, Aschauer M, Schäffler F, Abstreiter G and Gornik E 1994 *Solid-State Electron.* **37** 949

[11] Xie Y H, Monroe D, Fitzgerald E A, Silverman P J, Thiel F A and Watson G P 1993 *Appl. Phys. Lett.* **63** 2263

[12] Xie Y H, Fitzgerald E A, Monroe D, Silverman P J and Watson G P 1993 *J. Appl. Phys.* **73** 8364

[13] Ensslin K, Häusler K T, Lettau C, Lorke A, Kotthaus J P, Schmeller A, Schuster R, Petroff P M, Holland M and Ploog K 1992 *Low-Dimensional Electronic Systems—New Concepts* ed G Bauer *et al* (Berlin: Springer) p 45

[14] Thornton T J, Roukes M L, Scherer A and van de Gaag B P 1989 *Phys. Rev. Lett.* **63** 2128

[15] Müller G, Streda P, Weiss D, von Klitzing K and Weimann G 1994 *Phys. Rev.* B **50** 8938